Structural insights into pre-pore intermediates of alpha-hemolysin in the lipidic environment

Arnab Chatterjee[1$], Anupam Roy[1$], Thejas Satheesh[2], Partho Pratim Das[1], Bapan Mondal[1], Prithiv Kishore[1], Mahipal Ganji[2], Somnath Dutta[1#]

[1]Molecular Biophysics Unit, Indian Institute of Science, Bengaluru, India

[2]Department of Biochemistry, Indian Institute of Science, Bengaluru, India

[3]Department of Bioengineering, Indian Institute of Science, Bengaluru, India

[$]Equally contributed.

[#]Corresponding Author: Somnath Dutta, somnath@iisc.ac.in

Supplemental Figures and Legends

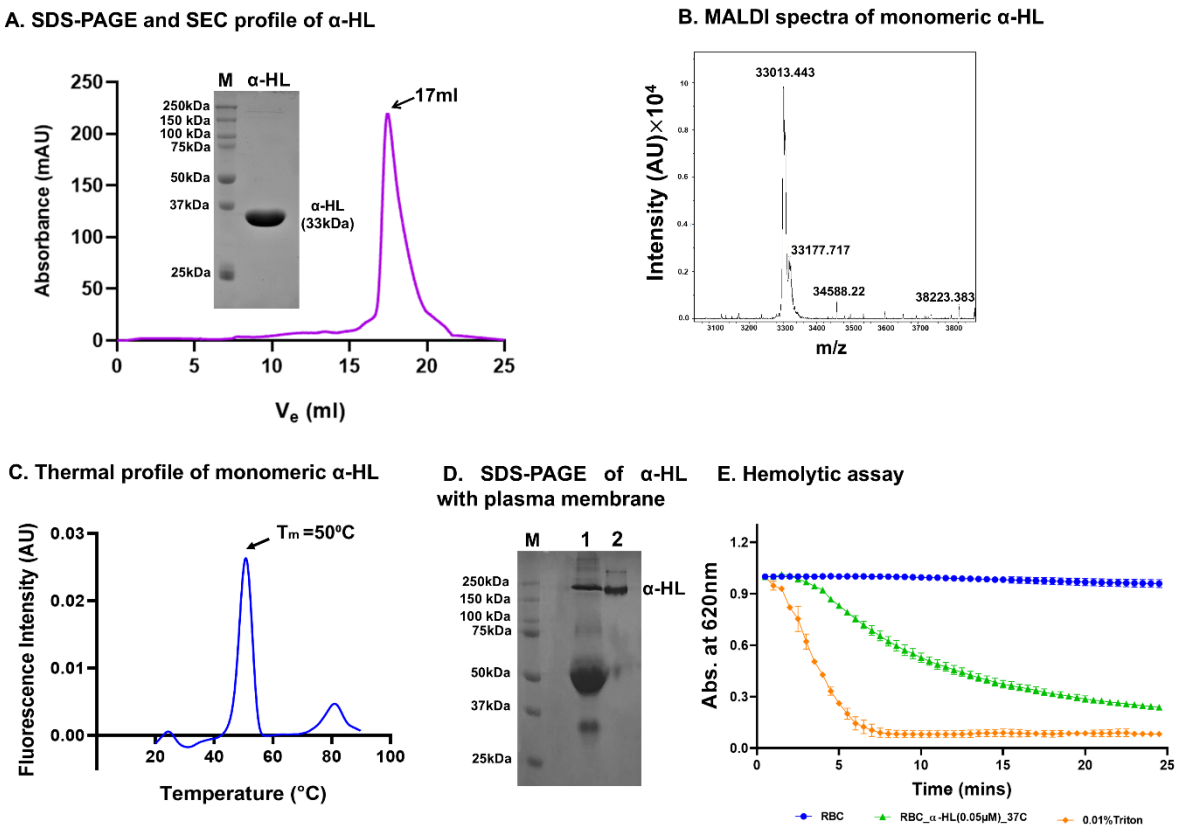

Figure S1: Preliminary purification and characterization of α-HL.

A. SDS-PAGE of SEC purified α-HL monomer. Size exclusion chromatography (Superdex™ S200 increase 10/300 GL) profile of recombinant α-HL monomer. ***B.*** *MALDI spectra analysis of recombinant α-HL showed a molecular weight of intact protein of ~33kDa.* ***C.*** *Thermal denaturation spectral profile of the monomeric toxin.* ***D.*** *SDS-PAGE profile of oligomeric protein contents presents in the supernatant fraction of α-HL treated rabbit erythrocytes (lane-2).* ***E.*** *Hemolytic assay of rabbit erythrocytes (10%) was performed with purified monomeric α-HL toxin (50 nM)*

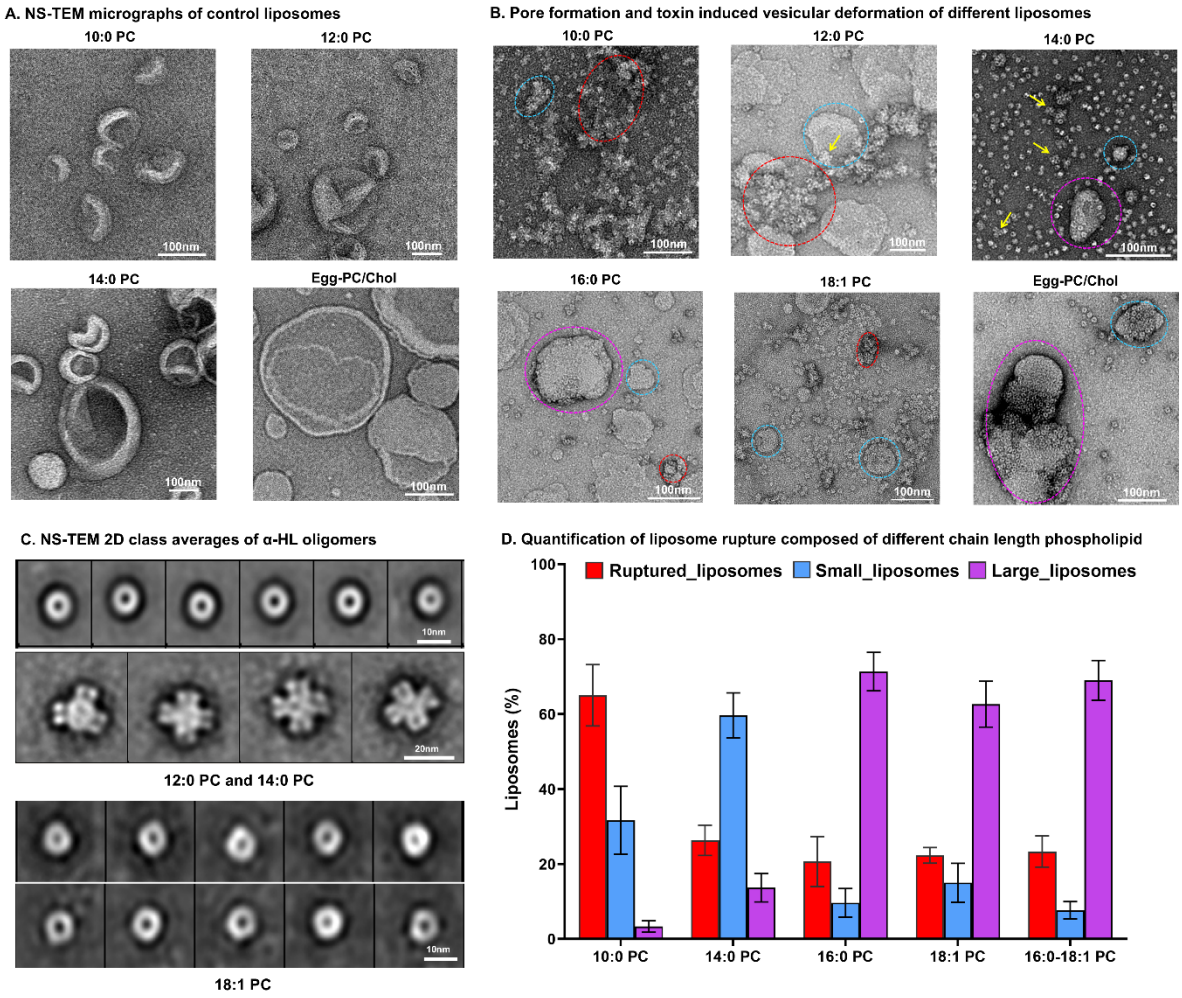

Figure S2: Different modes of toxin (α-HL) mediated lipid membrane re-modulations.

A*. NS-TEM micrographs of control liposomes (10:0, 12:0, 14:0, egg-PC/Chol).* ***B.*** *Change in liposome morphology of (10:0, 12:0, 14:0, 16:0, 18:1, and Egg-PC/Chol after toxin incubation shown encircled by cyan (large vesicles), violet (small lipid-protein cluster) and orange-red (ruptured lipid). Yellow arrow showed higher-order protein-lipid assembly.* ***C.*** *The representative NS-TEM 2D class averages of oligomeric states of α-HL (12:0, 14:0, and 18:1 PCs) and higher ordered oligomeric species (12:0 and 14:0PC).* ***D.*** *Comparison of liposome morphologies after toxin incubation is represented in bar plot.*

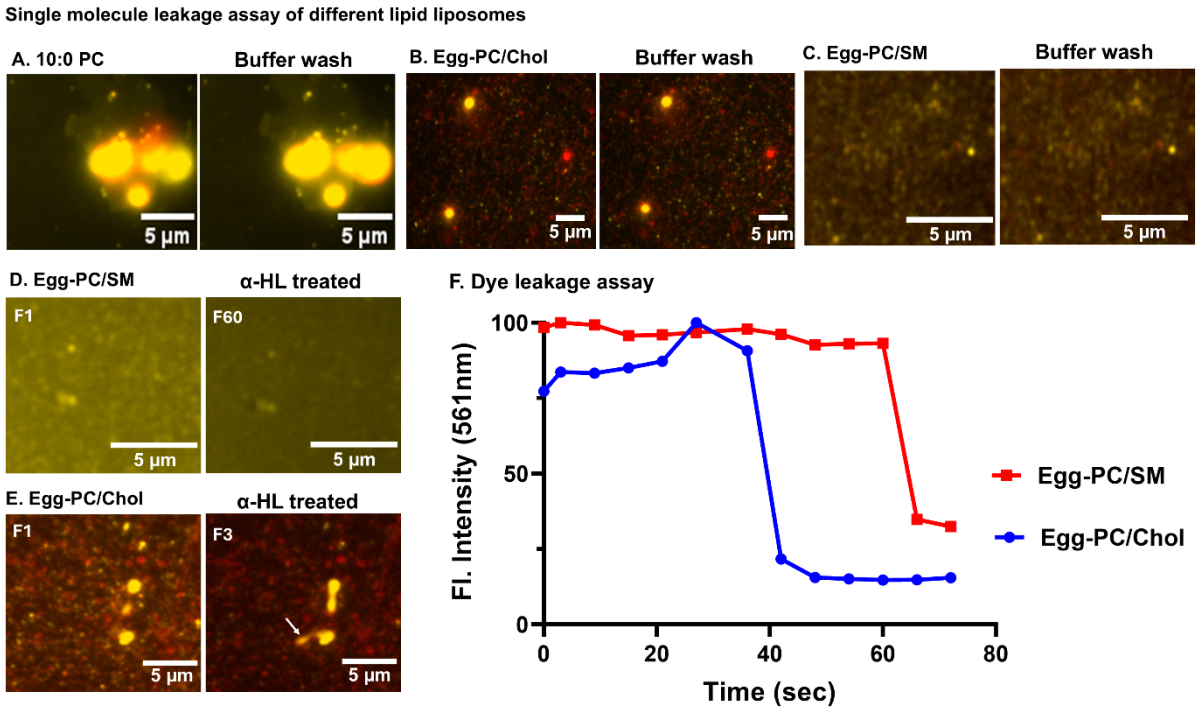

Figure S3: α-HL induced rhodamine leakage assay with different composites vesicles.

A-C. *The relative fluorescence intensities during Total Internal Reflection Fluorescence (TIRF) microscopic imaging for both fluorophores remained unchanged while washing with buffer through the flow-channel-bound liposomes (lipid in red color and encapsulated dye in yellow color).* ***D.*** *Toxin-treated NBD-PE labelled Egg PC/SM liposomes shown in pseudo color (red), filled with rhodamine (in yellow), showed a decrease in the fluorescence of Rhodamine dye.* ***E.*** *Protrusion of Egg-PC/Chol liposomes after α-HL treatment (white arrow).* ***F.*** *Comparison of single-molecule based different composites vesicle encapsulated rhodamine leakage assay showed significant delays in the lag phage for their kinetics.*

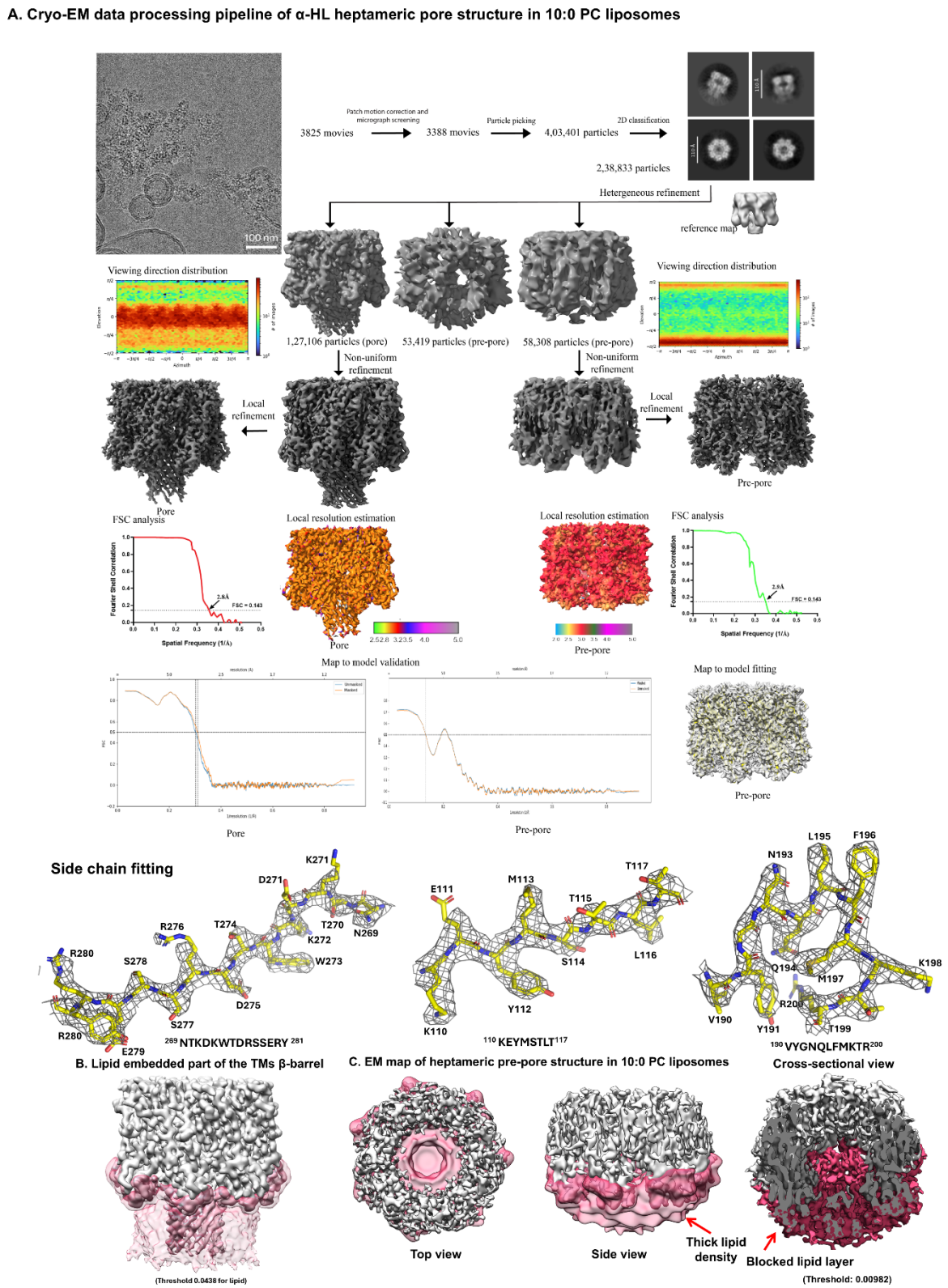

Figure S4: Cryo-EM data processing pipeline and maps of oligomeric species formed in the presence of 10:0 PC liposomes.

A. *Cryo-EM data processing pipeline for the oligomeric states of α-HL identified from 10:0 PC liposomes. Gold Standard FSC of heptameric pore and pre-pore cryo-EM map had a 2.8 Å and 2.9 Å global resolution respectively. An angular distribution and the local resolution distributions for both the cryo-EM maps of heptameric pore and pre-pore states were depicted. The electron density of the EM map was fitted with their respective atomic models (cartoon representations). Side chain fitting of residues is also shown.* ***B.*** *Lipid embedded part of pore structure is shown after low-pass filtering of*

lipid densities. ***C.*** *The top and bottom views of the heptameric pre-pore structure. A low-pass filtered thick lipid density (gray) completely blocked TMs pore vestibule.*

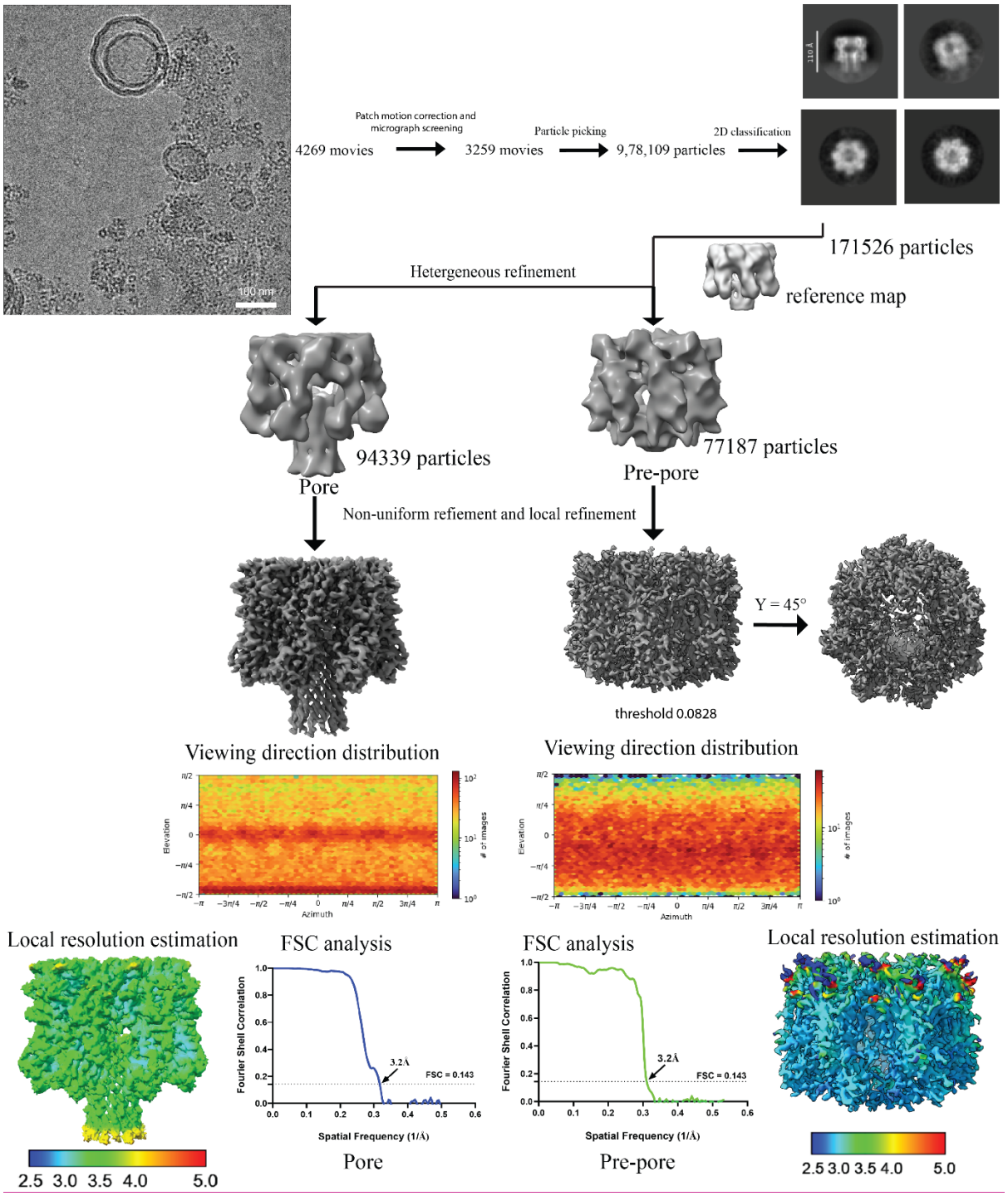

Figure S5: Cryo-EM data processing pipeline of heptameric conformations derived from 12:0 PC liposomes.

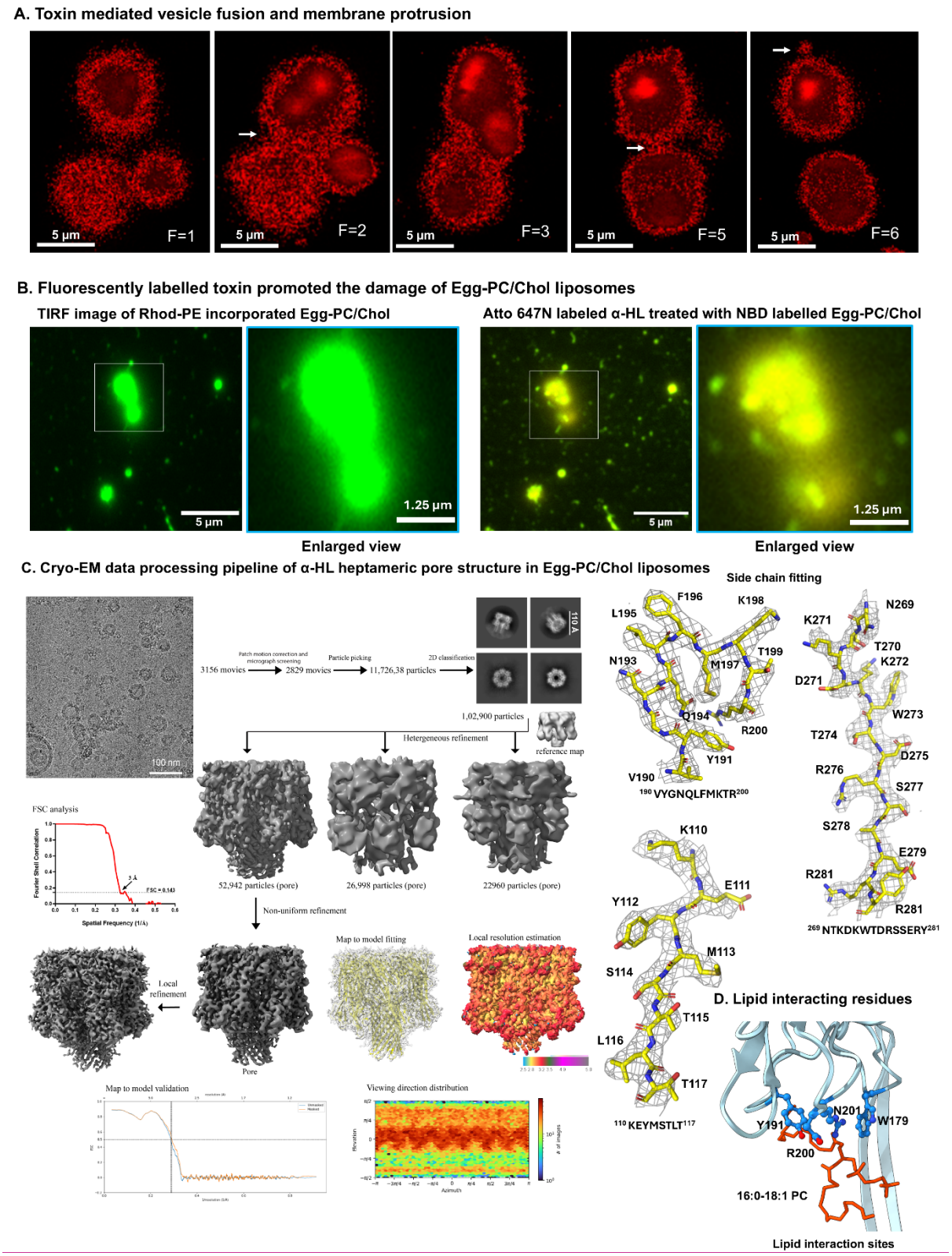

Figure S6: Impacts of toxin on composites lipid membranes and cryo-EM analysis of heptameric pore structure from Egg-PC/Chol liposomes.

A. *Snapshots of different fates of liposomes after toxin treatment including vesicle-vesicle fusions and protrusion of lipid bodies (white arrows).* ***B****. TIRF image showing a pseudo green fluorescence of Rhod-PE tagged Egg-PC/Chol liposomes (left). Binding and co-localization of atto488 fluorescent-tagged 278C α-HL (λ_{em}= 540 nm, yellow-colored) on Rhod-PE (λ_{em}= 580 nm) tagged Egg-PC/Chol liposome represented in an enlarged view (right).* ***C.*** *Cryo-EM data processing pipeline of α-HL heptameric pore structure isolated from Egg-PC/Chol liposomes.* ***D.*** *Amino acids of the rim domain interacting with 16:0/18:1 lipid chain are shown ball and stick.*

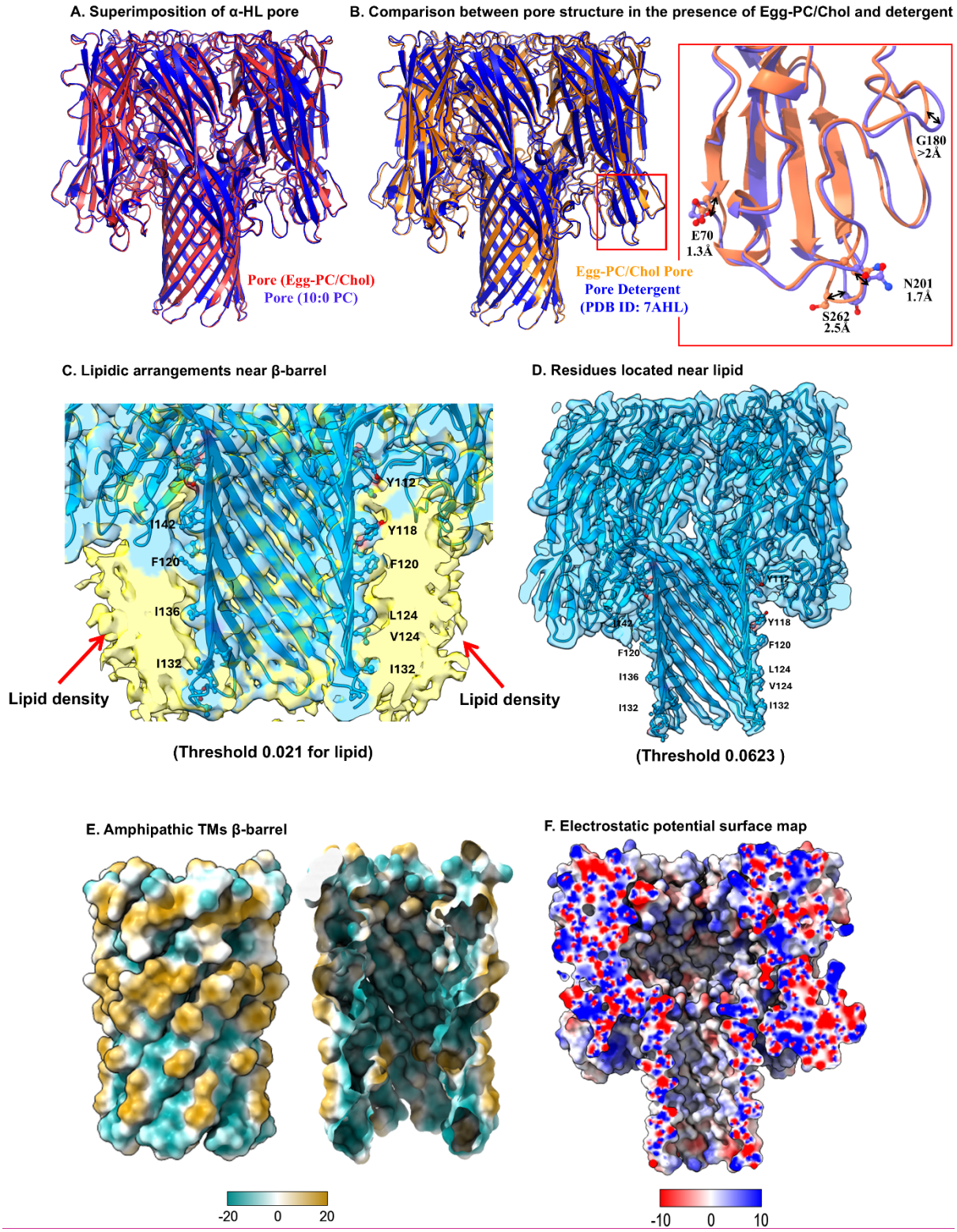

Figure S7: Structural overviews of heptameric α-HL pore conformation in different conditions and protein-membrane (lipid) interfaces.

A. *Structural superimposition of pore structure derived from egg PC/Chol and 10:0 PC lipid vesicles.* ***B.*** *Difference between detergent-derived and Egg PC/Chol-derived heptameric pore structure.* ***C.*** *Structural overview of extra lipid layer (yellow color) surrounding the transmembrane domain.* ***D.*** *The amphipathic aromatic residues Y112 (from β6) and Y148, H144 (from β7) located at upper TMs and hydrophobic residues L116, Y118, F120, and V140 located at upper TMs.* ***E.*** *The hydrophobic surface distribution of TMs pore predicted localization of hydrophobic side chain (golden) at upper TMs and polar residues (cyan) in lower TMs (left). While the cross-sectional of inner TMs pore was predominantly polar. Scale bar reflected the relative change in hydrophobic and polar distribution. Respective value in the bar showed the hydrophobicity index, where golden represents hydrophobic residues.* ***F.*** *Surface charge distribution of the inner cross-sectional part of the entire channel. Red color showing the negatively charged residues, while blue color showing positively charged residues.*

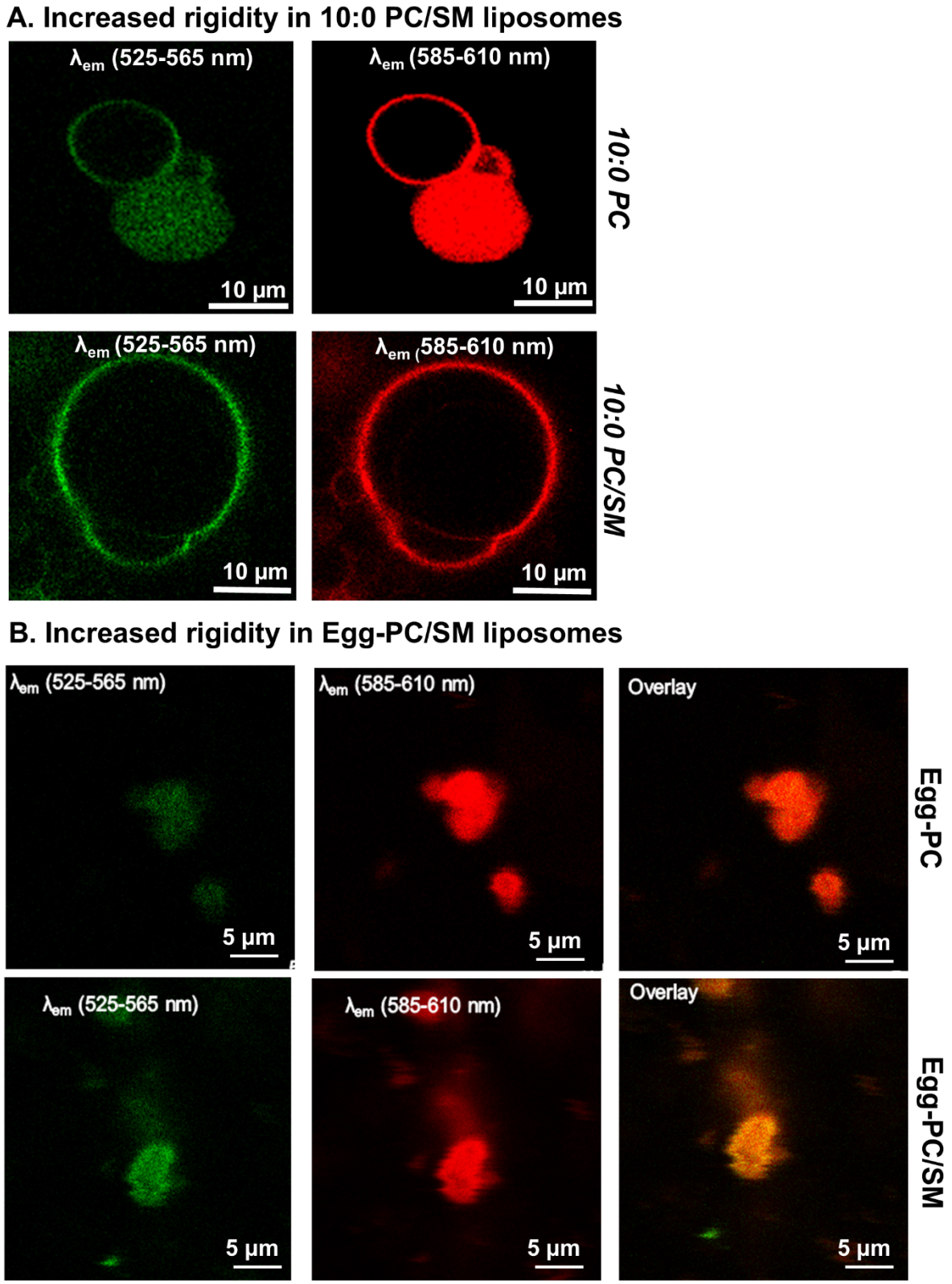

Figure S8: Impact of sphingomyelin on membrane rigidity.

A. *Confocal images of 10:0 PC and 10:0-PC/SM in the presence of lipophilic membrane staining dye Nile red.* ***B.*** *Confocal images of Egg-PC and Egg-PC/SM in the presence of lipophilic membrane*

staining dye Nile red. SM incorporated 10:0 PC, and Egg-PC showed a relatively higher emission intensity of Nile red at 525-565 nm (green color).

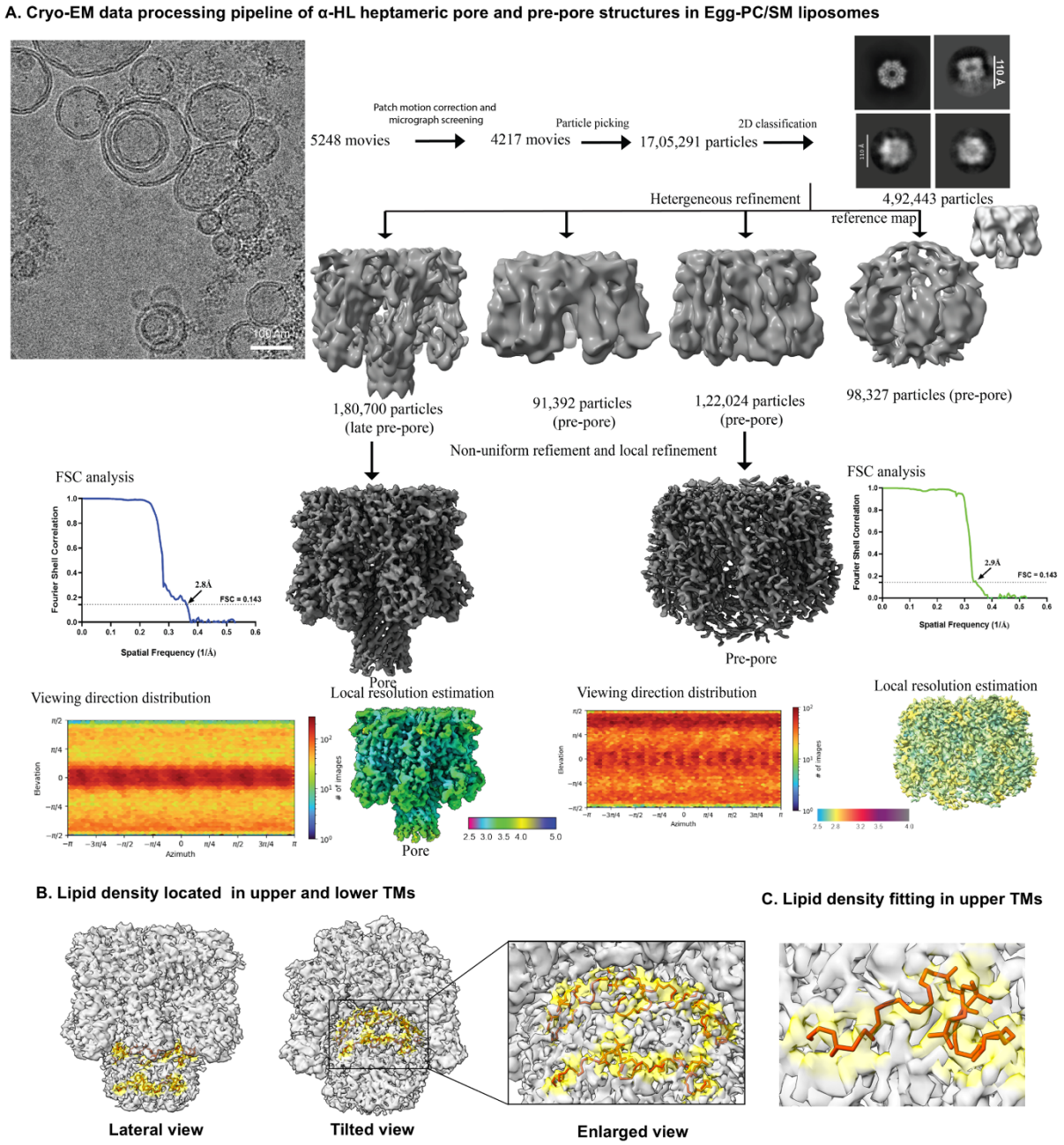

Figure S9: A. *Data processing pipeline of heptameric toxin derived from Egg-PC/SM liposomes.* ***B.*** *Location of lipid density at lower and upper TMs.* ***C.*** *Fitting of 16:0/18:1 lipid chain at the upper TMs.*

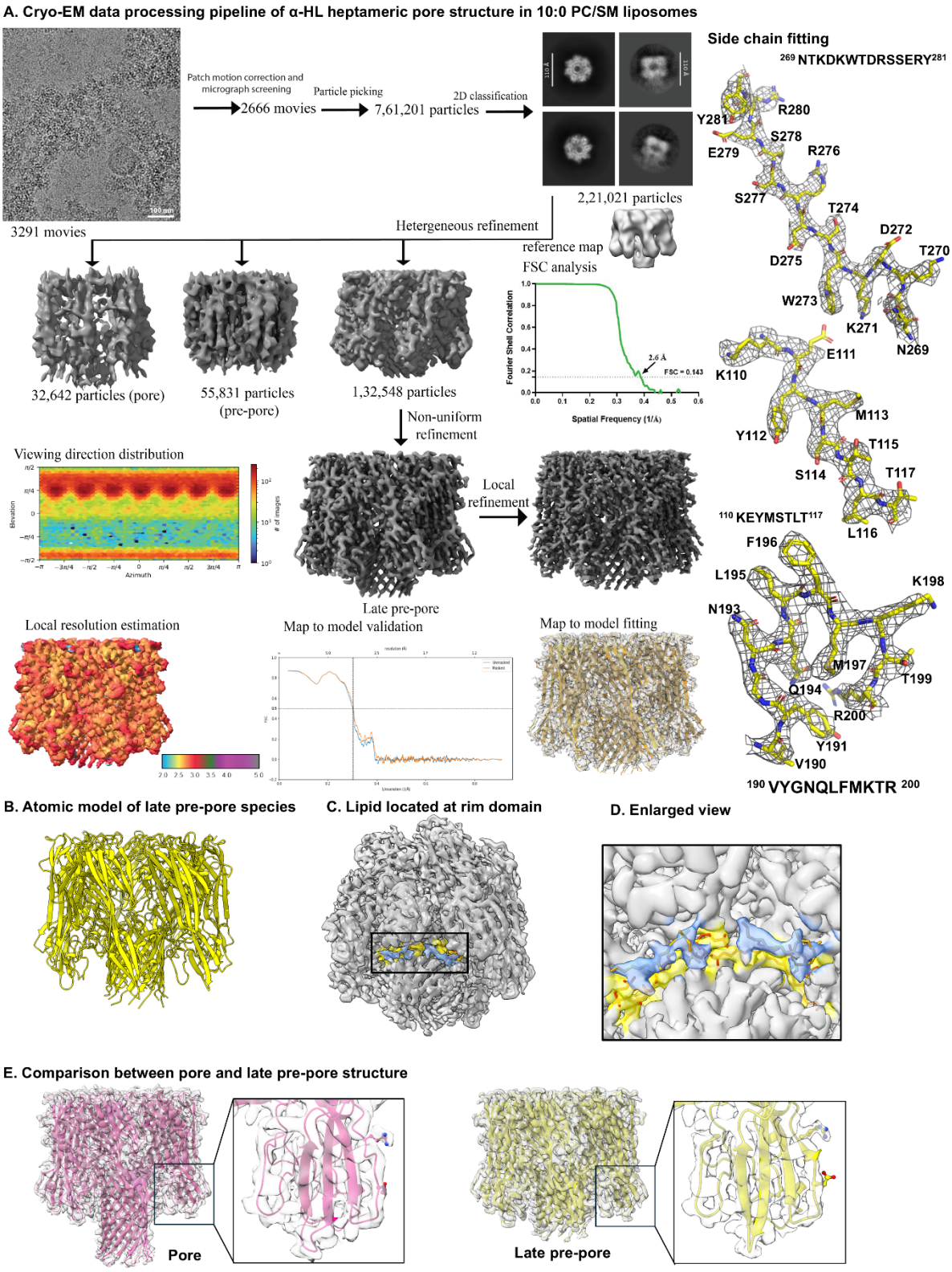

Figure S10. Cryo-EM data processing pipeline of α-HL heptamers derived from 10:0 PC/SM liposomes.

A. *Cryo-EM data processing pipeline for the oligomeric late pre-pore states of α-HL generated from 10:0 PC/SM liposomes.* ***B.*** *Atomic model of late pre-pore species.* ***C.*** *Lipid density located at the bottom of the rim domain.* ***D.*** *Enlarged of lipid location at rim and upper TMs.* ***E.*** *Map-to map comparison of 10:0 PC derived pore and 10:0 PC/SM derived late pre-pore with fitted atomic model Enlarged views showed density fitting at lower part of rim domain.*

Supplemental Information

Table S1: Cryo-EM Data collection, image processing, and refinement for membrane and α-HL structures.

Data Collection and Processing	**α-HL_10:0 PC**	**α-HL_10:0/SM**	**α-HL_Egg PC/Chol**	**α-HL_Egg PC/SM**	**α-HL_12:0 PC**
Magnification	54,000 X	54,000 X	54,000 X	54,000 X	54,000 X
Voltage	200 kV	200 kV	200 kV	200 kV	200 kV
Electron exposure ($e^-/Å^2$)	50	50	50	50	50
Defocus range (μm)	-1.25 to -2.75	-1.25 to -2.75	-1.25 to -2.75	-1.25 to -2.75	-1.25 to -2.75
Pixel size (Å)	0.92	0.92	0.92	0.92	0.92
Symmetry Imposed	C7	C7	C7	C7	C7
Number of micrographs	3825,	3291	3156	5248	4269
Number of particles	127106, 58308	132548	52942	180700, 122024	94339, 77187
Map Resolution (Å)	2.8, 2.9	2.6	3	2.8, 2.9	3.2, 3.2
FSC threshold	0.143	0.143	0.143	0.143	0.143
Map Resolution Range	2.5-4	2-4	2.5-4	2.5-4	2.5-5

Heptameric conformation	Pore and Pre-pore	Late pre-pore	Pore	Pore and Pre-pore	Pore and Pre-pore

Table S2: Cryo-EM map and model validation for membrane and α-HL structure.

_				
Validation	**10:0 PC(Pore)**	**10:0 PC (Pre-pore)**	**10:0 PC/SM (Late pre-pore)**	**Egg PC (Pore)**
MolProbity Score	2.05	2.97	1.7	1.63
Clash Score	16.96	25.78	5.98	5.75
Rotamer Outliers (%)	2.48	3.34	0.40	0.50
Ramachandran Plot			_	
Outlier (%)	0.00	0.12	0.10	0.10
Allowed (%)	2.06	15.70	5.28	4.42
Favored (%)	97.94	84.19	94.62	95.48

Table S3: Primer information.

Primer Name	Primer Sequence
HL_4RES_FR	5’-GGAATTCCATATGATTAATATCAAGACCGGCACCACC-3’
HL_9RES_FP	5’-GGAATTCCATATGGCACCACCGATATTGGCAG-3’
HL_TER_RP	5’-CCGCATATGATTGGTCATTTCCTCTTTTTCCC-3’
HL_278C_FP	5’-GATAAATGGACCGATCGTTGTAGCGAACGTTATAAAATTG-3’
HL_278C_RP	5’-CAATTTTATAACGTTCGCTACAACGATCGGTCCATTTATC-3’
HL_179W_FP	5’-GGTTAACCAGAACTGGGGTCCGTATGATCG-3’
HL_179W_RP	5’-CGATCATACGGACCCCAGTTCTGGTTAACC-3’
HL_200R_FP	5’-GCTGTTTATGAAAACCCGTAATGGCAGTATGAAAGC-3’
HL_200R_RP	5’-GCTTTCATACTGCCATTACGGGTTTTCATAAACAGC-3’

Table S4: Reagent and source information.

REAGENT	SOURCE	IDENTIFIER
Bacterial and virus strains		
***Escherichia coli* BL21(DE3)**	Novagen	Cat# 69450-3CN
Chemicals, peptides, and recombinant proteins		
Tris Base	HiMedia	Cat# TC072M
Sodium Chloride	Qualigens	Cat# Q15918
Potassium Chloride	Merck	Cat# P3911
Potassium di-hydrogen orthophosphate	Qualigens	Cat# Q19465
Di-sodium hydrogen orthophosphate	SD Fine Chemicals	Cat# S40158 K05
Luria Broth	HiMedia	Cat# M575
Isopropyl ß-D-1-thiogalactopyranoside	Merck	Cat# I6758
Imidazole	Sigma Aldrich	Cat# 792527-500G
2-Methyl-2,4-pentanediol	Sigma Aldrich	Cat# 8208190100
L-α-phosphatidylcholine (Egg, Chicken)	Avanti Polar Lipids	Cat# 840051P-200mg
Cholesterol	Merck Millipore	Cat# C8997-5G
Ni-NTA Agarose	Qiagen	Cat# 30210
Coomassie Brilliant blue R 250	Merck	Cat# 1.12553
Precision Plus Protein™ Dual Color Standards	Bio-Rad	Cat# #1610374
Amicon Ultra-4 Centrifugal filter unit (10K)	Merck	Cat# UFC801024
PC Membranes 0.2µm	Avanti Polar Lipids	Cat# 610006-1EA
10mm Filter Supports	Avanti Polar Lipids	Cat# 610014-1EA
Extruder Set with Holder/Heating Block	Avanti Polar Lipids	Cat# 610000-1EA
Syringe (1000 µL)	Avanti Polar Lipids	Cat# 610017-1EA
DSPE-PEG (2000) Biotin	Avanti Polar Lipids	Cat#880129P-10mg
Brain SM	Avanti Polar Lipids	Cat#860062P-25mg
10:0 PC	Avanti Polar Lipids	Cat#853025P-25mg
14:0 PC (DMPC)	Avanti Polar Lipids	Cat#850345C-500mg
16:0 PC (DPPC)	Avanti Polar Lipids	Cat#850355C-500mg
18:1(Δ9-Cis) PC (DOPC)	Avanti Polar Lipids	Cat#850375P-1g
Rhodamine B	Sigma-Aldrich	Cat#83689-1G
Nile-Red	Sigma-Aldrich	Cat#72485-100MG
4ME 16:0 NBD PE (NBD-DPhPE)	Avanti Polar Lipids	Cat#810142C-1mg
Streptavidin		
Egg Liss Rhod PE	Avanti Polar Lipids	Cat#810146C-5mg
Egg PC	Avanti Polar Lipids	Cat#131601P-5g
Uranyl Acetate 98%, ACS Reagent	Polysciences, Inc	Cat# 21447-25
Superdex 200 Increase 10/300 GL	Cytiva	Cat# GE28-9909-44
EM grid (Carbon film 300 mesh, Copper)	Electron Microscopy Sciences	Cat# CF300-CU
EM grid (Quantifoil R 1.2/1.3 300 Mesh, Copper)	Electron Microscopy Sciences	Cat# Q3100CR1.3
Quantifoil R 1.2/1.3, UT, 300 Mesh, Copper	Electron Microscopy Sciences	Cat# Q3100CR1.3-2nm
4',6-diamidino-2-phenylindole	Thermofisher Scientific	Cat#D1306
Atto 647N Maleimide	Sigma Aldrich	Cat#05316
Streptavidin	Sisco Research Laboratories	Cat#87610